



Removal of Cationic Dye from Aqueous Solution Using Agricultural Wastes: Argan and Almond Shells

M. El-khomri, N. El-messaoudi, S. Bentahar, A. Dbik, A. Lacherai*

Laboratory of Applied Chemistry and Environment, Department of Chemistry, Faculty of Science, University Ibn Zohr, Agadir, Morocco

PAPER INFO

Paper history:

Received 14 October 2018

Accepted in revised form 31 December 2018

Keywords:

Adsorption isotherm
Dye removal
biosorption
Agro waste
water treatment

ABSTRACT

In this work, Crystal Violet (CV), cationic dye, is removed from aqueous solution, using wood of Argan shell (ARS) and Almond shell (ALS), as low-cost and eco-friendly biosorbents. The parameters influencing the adsorption of CV on each of our adsorbents, contact time (5–180 min), adsorbent dose (0.2–2 g), pH of the solution (3–11), temperature (20–50°C) and the initial dye concentration (50–500 mg.L⁻¹), were investigated. The modeling of experimental results obtained, showed that the CV adsorption on both biomaterials followed a pseudo-second-order kinetic and in perfect agreement with Langmuir isotherm. Also, at 40 °C, CV is better adsorbed on ALS than ARS, with maximum biosorption amounts 51.99 mg.g⁻¹ and 37.32 mg.g⁻¹, respectively. Thermodynamic calculations have shown that the sorption is spontaneous, endothermic and random at the solid / solution interface. Adsorption capacities of dyes by ARS and ALS were better or comparable to those of several other biomaterials already studied. ALS and ARS biomaterials studied can be considered as alternative biosorbents low-cost and eco-friendly.

doi: 10.5829/ijee.2018.09.04.05

INTRODUCTION

Water, this simple molecule, source of life on earth: the blue planet thanks to these $\frac{3}{4}$ covered by this noble matter. Despite this abundance, the united nation count more than 700 million people who have not yet improved drinking water sources and 82% of them live in rural areas [1]. This situation is caused mainly by the lack of water resources and the pollution as well. In recent decades, industrial activities have developed rapidly, generating more and more quantities of pollutants. This problem is much more serious in the developing countries, in which its pollutants are discharged directly into the sanitation networks without any treatment.

Textile, plastics, food, pharmaceutical and paper industries use large quantities of organic dyes to dye their product, but 40000-50000 tons of dyes are continuously entering into the water systems [2]. The presence of these dyes in aquatic environments even in small quantities is misadvised, because the majority of them are toxic, carcinogenic, and mutagenic. Also, their presence imbalances aquatic environments by inhibiting access to light absorbed by phytoplankton and hydrophytes, reducing photosynthesis, and concentration of dissolved oxygen in the aquatic environment, which causes an increase of the chemical oxygen demand (COD) level [3]. Thus the removal of dyes

from wastewater is an important challenge to the survival of humanity.

Dyes are classified according to their charges on cationic, anionic, and non-ionic dyes. Generally, cationic dyes are the most toxic one [4]. Crystal violet is one of them, used in a variety of ways: as a biological stain, dermatological agent, veterinary medicine, additive to poultry feed to inhibit propagation of mould, intestinal parasites and fungus, textile dyeing and paper printing etc. [5]. However, CV is also a mutagen and mitotic poison which justified the choice of crystal violet as pollutants in the present study. The most common and famous methods which used for wastewater treatment are oxidative degradation [6], photo degradation [7], electro coagulation [8], biochemical degradation [9], anaerobic/aerobic treatment [10], coagulation/flocculation [11], membrane separation [12] and sorption [13]. Despite this multitude of choices, many of them remain applicable on a large scale due to cost problem and process complexity [13, 14]. But adsorption can be an interesting alternative because this technique is efficient, economical, easy to develop, and valid for different pollutants [14]. The cost of this technique can be further optimized from other techniques by using new adsorbents based on agricultural waste instead of activated carbon.

In this study, we chose two materials that largely exist in

* Corresponding author: A. Lacherai
E-mail: a.lacherai@uiz.ac.ma

the region of Souss Massa (southern Morocco) outcome from the shell of Argan and almond tree as adsorbent in the treatment of wastewater loaded by CV, in order to value them by creating a new added value.

The adsorbents were characterized by Fourier transform infrared (FTIR) coupled by attenuated total reflectance (ATR) technique and Thermo gravimetric analysis (TGA).

Biosorption of CV on ARS and ALS was performed by varying parameters such as contact time, adsorbent dose, initial dye pH, temperature and initial dye concentration. Biosorption kinetic of CV was tested by the pseudo-first-order and pseudo-second-order models. The behavior of the equilibrium sorption was investigated through using Langmuir, Freundlich and Temkin isotherm models, and thus calculated thermodynamic parameters.

MATERIAL AND METHOD

Adsorbate preparation

In this study, we chose crystal violet as a pollutant to test the effectiveness of our adsorbents, CV is a cationic dye belonging to the family of triphenylmethanes, with chemical formula $C_{25}H_{30}N_3Cl$ and its structure is given in Figure 1. All the solutions used were prepared by successive dilutions from a stock solution of 1 g.L^{-1} .

Adsorbent preparation and characterization

Nuts shells of Argan and Almond used in this study were obtained from the region of Agadir in southern Morocco during the harvest of 2016; these shells were cleaned and washed several times with distilled water to remove impurities, then dried for 24 hours in the oven at 105°C . The dried material is crushed and sieved to remove particles larger than $100 \mu\text{m}$. Finally, the powders obtained are stored in hermetically sealed glass bottles.

The powders of ARS and ALS are characterized by Fourier Transform Infrared Spectroscopy (FTIR) with resolution 4 cm^{-1} in a spectrometer Jasco 4100, coupled to ATR. The thermal stability of those biomass were studied with thermo gravimetric analysis (TGA) in the range of $25\text{--}600^\circ\text{C}$ with the heating rate of $10^\circ\text{C min}^{-1}$ at air atmosphere, using a differential thermal analyser Shimadzu D60.

Batch equilibrium experiments

The adsorption tests are carried out by placing adsorbent masses ranging from 0.2 to 2g at particles size $<100\mu\text{m}$, in contact with 50 ml of an aqueous solution of CV of concentration ranging from 50 to 500 mg.L^{-1} , for a contact time varying between 5 and 180min, in a thermostated bath at temperatures between 21 to 51°C . The effect of the solution

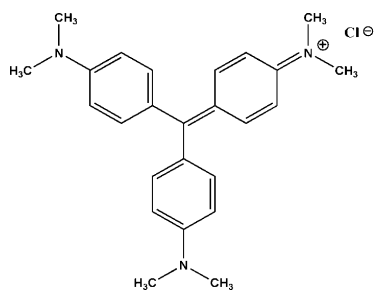


Figure 1. Chemical structure of crystal violet dye

pH is also sought by adjusting it to values between 3 and 11 by adding a few drops of HCl or NaOH (0.1M) solution before adsorption. It should be noted that throughout this study, and before measurement, all the samples were left in a centrifuge for 10 min at 3000 rpm to have clear solutions and thus obtain reproducible results. The residual amount of dye in each flask was determined using UV-Visible spectrophotometer "UV 2300" set to $\lambda_{\text{max}} = 584 \text{ nm}$ corresponding to the maximum absorption of CV.

The quantity equilibrium adsorbed $q_e(\text{mg.g}^{-1})$ and the percentage adsorption $R(\%)$ were calculated by Equations 1 and 2, respectively [15, 16]:

$$q_e = \frac{(C_0 - C_e)}{w} \times V \quad (1)$$

$$R(\%) = \frac{(C_0 - C_e)}{C_0} \times 100 \quad (2)$$

where, C_0 (mg L^{-1}) and C_e (mg L^{-1}) are the initial and equilibrium concentrations of CV, respectively. V (L) is the volume of solution and W (g) is the weight of adsorbent used.

RESULTS AND DISCUSSION

Characterization of adsorbents

a) FTIR spectroscopy

Figure 2 shows the vibrations of the functional groups presented on surface of ARS and ALS detected by FTIR. From the analysis of these spectra we can note the great resemblance in the chemical functions present in the surface of our adsorbents, also its complex surfaces, reflected by the very important number of peak. The most remarkable peaks are regrouped in Table 1.

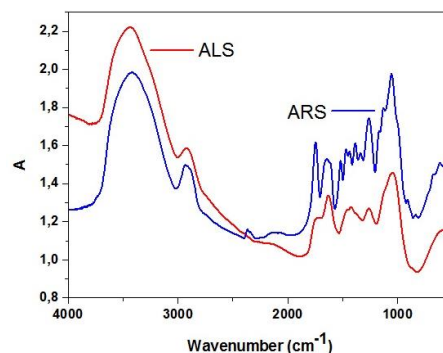


Figure 2. FTIR spectra of ARS and ALS

TABLE 1. The assignments corresponding to different frequencies observed in the FTIR spectra of ARS and ALS

| Frequency (cm^{-1}) | Assignment | Reference |
|--------------------------------|---|-----------|
| 3450 | -OH groups | [17] |
| 2900 | C-H aliphatic asymmetric stretching present in biomass structure (cellulose, hemicellulose, and lignin) | [18] |
| 1720 | C=O band | [19] |
| 1650 | C=O stretching | [20] |
| 1425 | due to aromatic ring of lignin | [21] |
| 1260 | the vibration C-O methoxy groups of lignin | [22] |
| 1150 | C-O-C vibration in cellulose and hemicellulose | [22] |
| 600 | -C-C- group | [20] |

b) Thermo gravimetric analysis TGA

The curves of TGA were carried out to investigate thermal decomposition behaviour of ARS and ALS, as shown in Figure 3. The analysis of TGA curves of ARS and ALS shows that both decompose thermally in four steps [23, 24]:

- The first step appears between 65°C and 120°C, this corresponds to the step of dehydration of the surface and the structure. During this stage there is a loss of approximately 10% of mass [25].
- The second step was in between 260°C and 350°C which may correspond to the thermal depolymerisation of hemicelluloses [26, 27], accompanied by a loss of 60% of the initial mass.
- The third step appears between 350°C and 450°C which corresponds to the degradation of cellulose [28], with 10% of mass loss.
- The latter step was in between 450 and 510°C which may be due to the decomposition of lignin [29] with a mass loss of nearly 20%.

c) Point of zero charge pH_{pzc}

The pH_{pzc} determines combined influence of all the functional groups of surface. In order to determine this parameter, a series of NaCl solutions (0.1M, 50mL) is used, the pH of each solution is adjusted, before contact with adsorbent, with a few drops of HCl/NaOH (0.1M) solution to have a series of pH_i ranging from 2 to 12. Then 0.5 g of one adsorbent is added to each solution, and the mixtures are stirred magnetically, after 24h of stirring, the final pH (pH_f) of each solution is measured. The pH_{pzc} is determined graphically by the intersection of the line ($pH_i = pH_f$) with the curve $pH_f = f(pH_i)$. The results are presented in Figure 4.

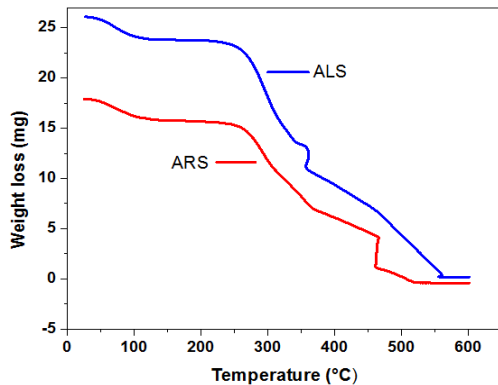


Figure 3. TGA curves of ARS and ALS

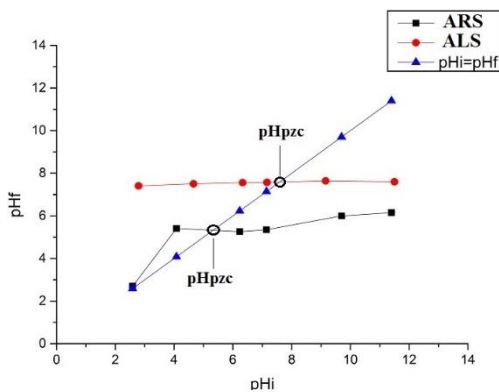


Figure 4. Point of zero charge pH_{pzc}

From Figure 4 we can observe that $pH_{pzc} = 5.5$ for ARS and 7.5 for ALS, so at $pH < pH_{pzc}$, the adsorbent surface has a net positive charge, while at $pH > pH_{pzc}$ surface has a net negative charge [30].

Adsorption study

a) Effect of adsorbent dose

The effect of adsorbent dose on adsorption is sought by adding masses of adsorbent ranging from 0.2 to 2 g in 50 mL of CV solution with initial concentration of 100 $mg.L^{-1}$, the CV and adsorbent mixture are allowed to stir for 60 min in a thermostated bath at 25°C. The results obtained are collated in Figure 5. This figure shows that the adsorption efficiency increases with the mass of adsorbent used to reach a plateau from 0.4 g. So 0.4 g of adsorbent is largely enough to eliminate almost 100% of CV.

b) Effect of contact time and kinetic study

In wastewater treatment, the time of a process is very important, a long time limit the amount of treated water per day, and increases the cost of the agitation. For this reason a very short time treatment is always desired. The effect of the adsorbate-adsorbent contact time is investigated by placing 0.4 g of adsorbent in 50 mL of CV solution (100 $mg.L^{-1}$) for time ranging from 5 min to 180 min. The results are presented in Figure 6.

As can be seen from Figure 6, 10 min of agitation is largely sufficient to eliminate almost 100% of pollutant. This rapidity shows the high affinity between CV and ARS and ALS. So in the rest of this work will be limited to 10 minutes of contact, which is a very short time compared to other studies (Table 2).

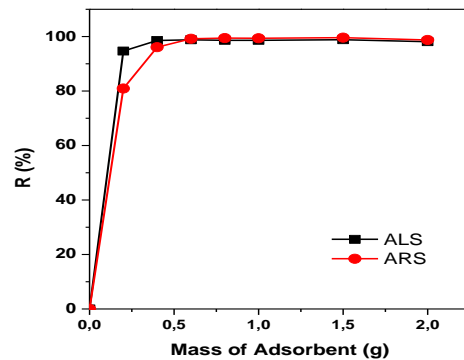


Figure 5. Effect of adsorbent dose on the adsorption of CV on ARS and ALS ($t = 60$ min, $C_0 = 100$ $mg.L^{-1}$; $T = 25$ °C)

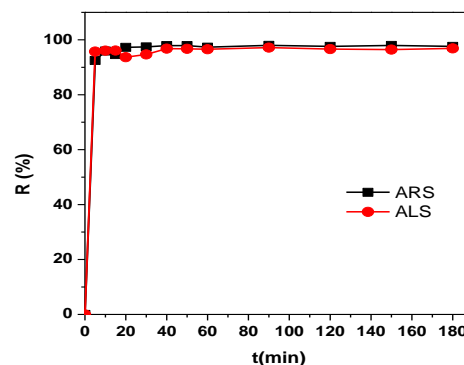


Figure 6. Effect of contact time on the adsorption of CV on ARS and ALS ($Ad = 8$ $g.L^{-1}$, $C_0 = 100$ $mg.L^{-1}$, $T = 25$ °C)

TABLE 2. The equilibrium contact time for adsorption of CV by different adsorbents

| Adsorbent | t(min) | Reference |
|--|--------|------------|
| Nano porous carbon from tomato paste waste | 150 | [31] |
| Treated ginger waste | 150 | [5] |
| Palm kernel fiber | 60 | [32] |
| CarAlg/MMt nano composite hydrogels | 120 | [33] |
| Materials bottom ash | 240 | [2] |
| Raw powder of jujube shell | 60 | [34] |
| Sugarcane dust | 14 | [35] |
| Peels of Annona squamosa | 60 | [36] |
| Pinus bark powder | 120 | [37] |
| ARS | 10 | This study |
| ALS | 10 | This study |

The modelling of this results by the kinetic models of first and pseudo second order, allowed us to determine the order and the rate of the reaction, by using the linear forms of these two models:

- Pseudo-first order model expressed by Lagergren equation [38], which can be linearized in the form of Equation 3:

$$\log(q_e - q_t) = \log q_e - \frac{K_1}{2.303} t \quad (3)$$

- Pseudo-second order model expressed and linearized in the form of Equation 4 [39]:

$$\frac{t}{q_t} = \frac{1}{K_2 q_e^2} + \frac{1}{q_e} t \quad (4)$$

where, q_e (mg.g^{-1}) and q_t (mg.g^{-1}) are the amounts of CV adsorbed respectively at equilibrium and at instant t , K_1 (min^{-1}) and K_2 ($\text{g.mg}^{-1}.\text{min}^{-1}$) are the rate constants of adsorption pseudo-first-order process and pseudo-second order.

The results of fitting experimental data with the pseudo first-order and pseudo second-order are presented in Table 3.

As can be seen, for both ARS and ALS, experimental data fitted well with the pseudo second-order model ($r^2 \approx 1$ and $q_{e,\text{calc}} \approx q_{e,\text{exp}}$). The calculated q_e values also agree very well with the experimental data. These results indicate that the adsorption system studied belongs to the pseudo second-order kinetic model.

c) Effect of initial concentration

Generally, the water in treatment plants comes from different sources, which leads to different concentrations to treat. In order to elucidate the effect of this parameter, aqueous solution loaded with CV at concentrations ranging between 50 and 500 mg.L^{-1} are stirred with 0.4 g of ARS or ALS for 10 min at natural pH. The results obtained are represented in

Figure 7. The analysis of these curves shows a yield decrease from 97.91% to 71.14% and from 98.92% to 46.17% for ALS and ARS, respectively. This decrease can be explained by the fact that at low concentration of CV there is a sufficient amount of active sites to trap most CV molecules. But when the initial concentration is increased the number of unadsorbed molecules increases implying a decrease in the adsorption yield of CV [13].

d) Effect of pH

Generally the pH of the medium plays an important role in the adsorption studies, because it can modify the dye molecules and also the chemical functions on the adsorbent surface. The results obtained are collated in Figure 8.

Figure 8 shows that the CV adsorbs on ARS and ALS in basic media better than in very acidic media. This can be justified by the fact that in acidic environments there is competition between H^+ and the CV which is also cationic, whereas in the basic media the dominance of HO^- tends to charge negatively the adsorbent surface, which promotes the adsorption of the CV [40]. This finding is in agreement with the pH_{pzc} results.

e) Effect of temperature and thermodynamic study

The effect of temperature on the adsorption of CV on ARS and ALS is carried out at 20, 30 and 40°C with initial concentration of CV varying from 50 to 500 mg.L^{-1} , and the results obtained are summarized in Figure 9.

Figure 9 shows a small increase in the amount of CV adsorbed on ARS and ALS with temperature, this small increase can be justified by the increase in the mobility of CV molecules with temperature [5]. The effect of temperature can be explained thermodynamically by the calculation of the variations of standard free enthalpy ΔG° , standard entropy ΔS° and standard enthalpy ΔH° . In the case of adsorption, these variations can be deduced from the Equations 5 and 6 [41]:

$$\Delta G^\circ = -RT \ln K_d \quad (5)$$

$$\ln K_d = \frac{\Delta S^\circ}{R} - \frac{\Delta H^\circ}{RT} \quad (6)$$

With K_d is the distribution coefficient defined by the Equation 7 [42]:

$$K_d = \frac{C_b}{C_s} \quad (7)$$

where, C_b (mg.L^{-1}) is the equilibrium dye concentration on the biosorbent and C_s is the equilibrium dye concentration in solution (mg.L^{-1}).

The values of ΔS° and ΔH° can be obtained by plotting $\ln K_d$ versus of $1/T$. The results are summarized in the following Table 4.

TABLE 3. Kinetic parameters for biosorption of CV onto ARS and ALS

| Adsorbent | $q_{e,\text{exp}}$ (mg.g^{-1}) | Pseudo-first order model | | | Pseudo-second order model | | |
|-----------|--|--|--------------------------------|-------|--|---|-------|
| | | $q_{e,\text{cal}}$ (mg.g^{-1}) | K_1 (min^{-1}) | r^2 | $q_{e,\text{cal}}$ (mg.g^{-1}) | K_2 ($\text{g.mg}^{-1}.\text{min}^{-1}$) | r^2 |
| ARS | 12.20 | 0.159 | 0.016 | 0.345 | 12.239 | 0.509 | 0.999 |
| ALS | 12.11 | 0.176 | 0.007 | 0.379 | 12.106 | 0.429 | 0.999 |

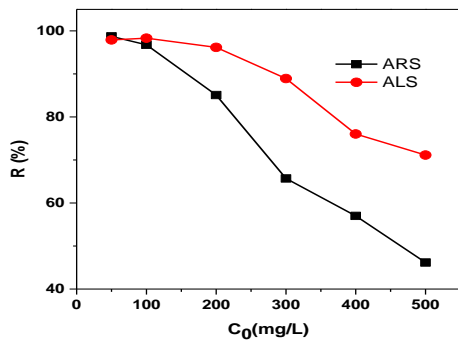


Figure 7. Effect of initial concentration on the adsorption of CV on ARS and ALS (Ad=8 g L⁻¹, t=10 min, T=20 °C)

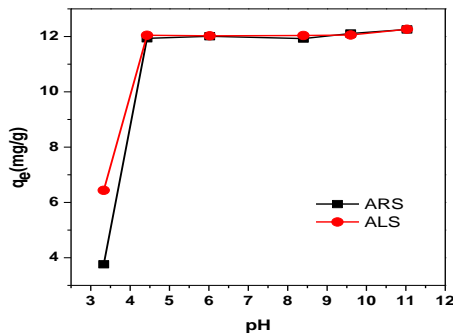


Figure 8. Effect of pH on adsorption of CV on ARS and ALS (Ad=8g L⁻¹, t = 10 min, T=25 °C, C₀=100 mg L⁻¹)

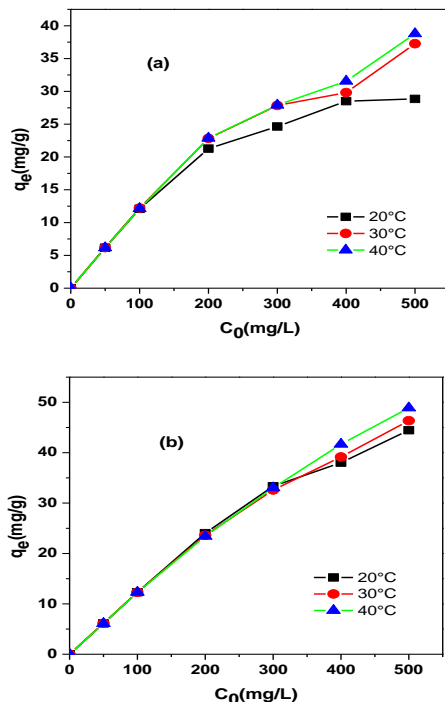


Figure 9. Effect of temperature on the adsorption of CV on ARS (a) and ALS (b)(Ad=8g.L⁻¹, t = 10 min, C₀ = 50-500 mg.L⁻¹).

From these results we can conclude that in this temperature range, the adsorption of the CV on ARS and ALS is thermodynamically possible ($\Delta G^\circ < 0$) and endothermic ($\Delta H^\circ > 0$). The positive value of ΔS° reflect the diminution of randomness at the solid / solution interface during the

TABLE 4. Thermodynamic study for the adsorption of CV on ARS and ALS (Ad=8 g L⁻¹, t = 10 min, C₀= 100 mg L⁻¹)

| Adsorbent | ΔG° (KJ mol ⁻¹) | | | ΔH° (KJ mol ⁻¹) | ΔS° (J mol ⁻¹ k ⁻¹) |
|-----------|--|--------|--------|--|---|
| | 293K | 303K | 313K | | |
| ARS | -11.82 | -11.95 | -11.83 | 11.93 | 17.43 |
| ALS | -11.19 | -11.72 | -11.59 | 17.46 | 18.98 |

adsorption process which can be explained by the fact that the adsorbed molecule will lose one translational degree of freedom (goes from 3D translation in solution to 2D translation on the solid surface), and also by a decrease in the dye concentration at the solid–solution interface [40, 41].

f) Adsorption isotherm

Adsorption isotherm is a relationship between C_e the adsorbate concentration in the liquid phase at equilibrium and q_e the amount of adsorbate trapped in the solid phase [43]. It provides useful information regarding the extent of affinity between the adsorbent surface and adsorbate molecules and also about the surface properties of adsorbent. Among the most used models in the literature to describe the experimental data, we quote Freundlich, Langmuir and Temkin models. In this work, we use those model in their linear forms expressed respectively with Equations 8 (Freundlich, 1906), 9 (Langmuir, 1918) and 10 (Temkin et al. 1940)[44, 45]:

$$\ln q_e = \ln K_F + \frac{1}{n} \ln C_e \quad (8)$$

$$\frac{C_e}{q_e} = \frac{1}{K_L q_m} + \frac{C_e}{q_m} \quad (9)$$

$$q_e = B \ln K_T + B \ln C_e \quad (10)$$

where q_m (mg.g⁻¹) is the theoretical maximum adsorption capacity; k_F, k_L, and k_T are the adsorption constants of Freundlich, Langmuir and Temkin models, respectively, 1/n is the intensity of the adsorption and B (J.mg⁻¹) is constant related to heat of sorption.

The equilibrium uptake data, obtained at 20, 30 and 40 °C, was applied to these models and the corresponding plots allowed us to determine the characteristic parameters of each one. The obtained results are summarized in Table 5.

From these results we can see on the one hand, that it is the Langmuir isotherm that best describes the adsorption of CV on our adsorbents, because the value of r² is always very close to 1, and in the other hand, that the operating conditions are favourable for CV adsorption on ARS and ALS according to the R_L value superior than 1. So we can conclude that the CV is adsorbed on a homogeneous adsorbent surface of identical sites that are equally available and energetically equivalent to each site carrying equal number of molecules and with no interaction between adsorbate molecules [46], with a maximum adsorption capacity of 37.32 mg.g⁻¹ for ARS and 51.99 m.g⁻¹for ALS.

The data presented in Table 6 compares the maximum monolayer adsorption capacity of some adsorbents used for the removal of CV.

As we can see that ARS and ALS shows a comparable adsorption capacity towards CV than that of most adsorbent.

TABLE 5. Isotherm parameters for the adsorption of CV onto ARS and ALS ($Ad=8\text{ g L}^{-1}$, $t=10\text{ min}$, $C_0=50\text{-}500\text{ mg L}^{-1}$)

| Adsorbent | T (°C) | Langmuir | | | Freundlich | | | Temkin | | |
|-----------|--------|-----------------------------|----------------------------|-------|------------|------|-------|--------|---------------------------|-------|
| | | q_m (mg.g ⁻¹) | K_L (L.g ⁻¹) | r^2 | K_F | n | r^2 | K_T | B (J.mg ⁻¹) | r^2 |
| ARS | 20°C | 29.39 | 123.02 | 0.996 | 7.95 | 4.02 | 0.963 | 7.72 | 3.82 | 0.994 |
| | 30°C | 35.20 | 109.38 | 0.974 | 8.57 | 3.64 | 0.954 | 6.19 | 4.72 | 0.965 |
| | 40°C | 37.32 | 90.08 | 0.973 | 7.84 | 3.30 | 0.958 | 3.66 | 5.35 | 0.966 |
| ALS | 20°C | 44.78 | 127.29 | 0.991 | 8.65 | 2.84 | 0.900 | 2.89 | 7.19 | 0.987 |
| | 30°C | 47.12 | 102.27 | 0.984 | 8.39 | 2.75 | 0.950 | 2.64 | 7.42 | 0.984 |
| | 40°C | 51.99 | 80.80 | 0.980 | 7.57 | 2.44 | 0.942 | 1.74 | 8.67 | 0.969 |

TABLE 6. Comparison of maximum monolayer adsorption capacity of CV by some adsorbents

| Adsorbent | q_m (mg g ⁻¹) | Reference |
|--|-----------------------------|------------|
| Nano porous carbon from tomato paste waste | 68.97 | [31] |
| Palm kernel fiber | 78.91 | [32] |
| CarAlg/MMt nano composite hydrogel | 88.84 | [33] |
| Date stones | 83.33 | [34] |
| Tomato plant root | 94.33 | [47] |
| Pinus bark powder | 32.80 | [37] |
| Wood apple | 19.81 | [5] |
| Sugarcane dust | 3.87 | [35] |
| Neem sawdust | 3.86 | [48] |
| Jujube shell | 59.84 | [34] |
| ARS | 37.33 | This study |
| ALS | 51.99 | This study |

CONCLUSION

In this study we showed that we can use ARS and ALS as a simple and economical adsorbent in the treatment of wastewater loaded with Crystal violet. Indeed, the maximum adsorption capacity obtained for ARS and ALS, which are of the order respectively of 37.33 mg.g⁻¹ and 51.9 mg.g⁻¹, are much greater or comparable to that obtained for other biomaterials. Also for both supports the adsorption of CV is fast (10 min), spontaneous, endothermic, follows a kinetics of pseudo second order and better described by the isotherm of Langmuir.

ACKNOWLEDGEMENTS

This research did not receive any specific grant from funding agencies in the public, commercial, or not for profit sectors.

REFERENCES

- Nations Unies, 2014. Objectifs du Millénaire pour le développement, Rapport 2014.
- Mittal, A., J., Mittal, A., D., Malviya, Kaur, and V. K., Gupta, 2010. Adsorption of hazardous dye crystal violet from wastewater by waste materials. *Journal of Colloid and Interface Science*, 343(2): 463-473.
- EL Khomri, M., A., EL Lacherai, and N., Messaoudi, 2014. Retention of Methylene Blue on an Agro-Source Material. *International Journal of Engineering Research & Technology*, 3: pp. 1657–1663.
- Hao, O.J., H., Kim, and P., Chiang, 2000. Decolorization of Wastewater. *Critical Reviews in Environmental Science and Technology*, 30: pp. 449–505.
- Kumar, R., R., Ahmad, 2011. Biosorption of hazardous crystal violet dye from aqueous solution onto treated ginger waste (TGW). *Desalination*, 265: 112–118.
- Menendez, A., J.I., Lombraña, and A., De Luis, 2011. Lumped-intermediates analysis in the photooxidation of Rhodamine 6G in the H₂O₂/UV system. *Korean Journal of Chemical Engineering*, 28: 388–395.
- Ariyanti, D., M., Maillot, and W., Gao, 2018. Photo-assisted degradation of dyes in a binary system using TiO₂ under simulated solar radiation. *Journal of Environmental Chemical Engineering*, 6(1): 539-548.
- Kalyani, K.S.P., N., Balasubramanian, and C., Srinivasakannan, 2009. Decolorization and COD reduction of paper industrial effluent using. *Chemical Engineering Journal*, 151: 97–104.
- Kagalkar, A. N., U. B., Jagtap, J. P., Jadhav, V. A., Bapat, and S.P., Govindwar, 2009. Biotechnological strategies for phytoremediation of the sulfonated azo dye Direct Red 5B using *Blumea malcolmii* Hook. *Bioresource technology*, 100(18): 4104-4110.
- Chinwetkitvanich, S., M., Tuntoolvest, and T., Panswad, 2000. Anaerobic decolorization of reactive dyebath effluents by a two-stage UASB system with tapioca as a co-substrate. *Water*

- Research, 34: 2223–2232,
11. Neamtu, M., A., Yediler, I., Siminiceanu, M., Macoveanu, and A., Kettrup, 2004. Decolorization of disperse red 354 azo dye in water by several oxidation processes—a comparative study. *Dyes and pigments*, 60(1): 61-68.
 12. Ciardelli, G., L., Corsi, and M., Marcucci, 2000. Membrane separation for wastewater reuse in the textile industry. *Resources, Conservation and Recycling*, 31: 189–197.
 13. Salleh, M.A.M., D.K., Mahmoud, W.A.W.A., Karim, and A., Idris, 2011. Cationic and anionic dye adsorption by agricultural solid wastes: A comprehensive review. *Desalination*, 280: 1–13.
 14. Sulak, M.T., E., Demirbas, and M., Kobya, 2007. Removal of Astrazon Yellow 7GL from aqueous solutions by adsorption onto wheat bran. *Bioresource Technology*, 98: 2590–2598.
 15. Ning-chuan, F., G.U.O., Xue-yi, and L., Sha, 2009. Enhanced Cu (C) adsorption by orange peel modified with sodium hydroxide. *Transactions of Nonferrous Metals Society of China*, 20: s146–s152.
 16. Pavan, F. A., E. S., Camacho, E. C., Lima, G. L., Dotto, V. T., Branco, and S. L., Dias, 2014. Formosa papaya seed powder (FPSP): preparation, characterization and application as an alternative adsorbent for the removal of crystal violet from aqueous phase. *Journal of Environmental Chemical Engineering*, 2(1): 230-238.
 17. Basrur D., and J.I., Bhat, 2017. Activated Carbon from Fenugreek Seed : Characterization and Dyes Adsorption Properties. *Iranian Journal of Energy & Environment*, 8: 127–135.
 18. El Messaoudi, N., M., El Khomri, S., Bentahar, A., Dbik, and A., Lacherai, 2016. Removal of crystal violet by biosorption onto date stones. *Scientific Study & Research. Chemistry & Chemical Engineering, Biotechnology, Food Industry*, 17(2): 151-167.
 19. Narvekar, A.A., J.B., Fernandes, and S.G., Tilve, 2018. Adsorption behavior of methylene blue on glycerol based carbon materials. *Journal of Environmental Chemical Engineering*, 6: 1714–1725.
 20. Nasuha, N., B.H., Hameed, and A.T.M., Din, 2010. Rejected tea as a potential low-cost adsorbent for the removal of methylene blue. *Journal of Hazardous Materials*, 175: 126–132.
 21. Pavan, F.A., E.C., Lima, S.L.P., Dias, and A.C., Mazzocato, 2008. Methylene blue biosorption from aqueous solutions by yellow passion fruit waste. *Journal of Hazardous Materials*, 150: 703–712.
 22. Al-Ghouti, M.A., A., Hawari, and M., Khraisheh, 2013. A solid-phase extractant based on microemulsion modified date pits for toxic pollutants. *Journal of Environmental Management*, 130: 80–89.
 23. Fateh, T., 2012. Etude expérimentale et numérique de la cinétique de décomposition thermique de contreplaqués en bois (Doctoral dissertation, ISAE-ENSMA. Ecole Nationale Supérieure de Mécanique et d'Aérotechnique - Poitiers, France).
 24. Bohnke, I., 1993. Étude expérimentale et théorique des traitements thermiques du bois . Caractérisation physico-mécanique des bois traités (Doctoral dissertation, L'Ecole Nationale Supérieure des Mines de Saint-Etienne).
 25. Bentahar, S., A., Lacherai, A., Dbik, and N., El-Messaoudi, 2015. Equilibrium , Isotherm , Kinetic and Thermodynamic Studies of Removal of Crystal Violet by Adsorption onto a Natural Clay. *Iranica Journal of Energy & Environment*, 6(4): 260–268.
 26. Essabir, H., S., Nekhlaoui, M., Malha, M. O., Bensalah, F. Z., Arrakhiz, A., Qaiss, and R., Bouhfid, 2013. Bio-composites based on polypropylene reinforced with almond shells particles: mechanical and thermal properties. *Materials & Design*, 51: 225-230.
 27. Arrakhiz, F. Z., M., El Achaby, K., Benmoussa, R., Bouhfid, E. M., Essassi, and A., Qaiss, 2012. Evaluation of mechanical and thermal properties of Pine cone fibers reinforced compatibilized polypropylene. *Materials & Design*, 40: 528-535.
 28. Ouajai, S., and R.A., Shanks, 2005. Composition, structure and thermal degradation of hemp cellulose after chemical treatments. *Polymer Degradation and Stability*, 89: 327–335.
 29. Albano, C., J., González, M., Ichazo, and D., Kaiser, 1999. Thermal stability of blends of polyolefins and sisal fiber. *Polymer Degradation and Stability*, 66: 179–190.
 30. Güzel, F., H., Saygılı, G.A., Saygılı, and F., Koyuncu, 2014. Decolorisation of aqueous crystal violet solution by a new nanoporous carbon: Equilibrium and kinetic approach. *Journal of Industrial and Engineering Chemistry*, 20: 3375–3386.
 31. Sayg, H., and F., Gu, 2014. Decolorisation of aqueous crystal violet solution by a new nanoporous carbon : Equilibrium and kinetic approach. *Journal of Industrial and Engineering Chemistry*, 20: 3375–3386.
 32. El-Sayed, G.O., 2011. Removal of methylene blue and crystal violet from aqueous solutions by palm kernel fiber. *Desalination*, 272: 225–232.
 33. Mahdavinia, G. R., H., Aghaie, H., Sheykhloie, M. T., Vardini, and H., Etemadi, 2013. Synthesis of CarAlg/MMT nanocomposite hydrogels and adsorption of cationic crystal violet. *Carbohydrate polymers*, 98(1): 358-365.
 34. El Messaoudi, N., M., El Khomri, A., Lacherai, S., Bentahar, A., Dbik, and B., Bakiz, 2017. Valorization and characterization of wood of the jujube shell: application to the removal of cationic dye from aqueous solution. *Journal of Engineering Science and Technology (JESTEC)*, 12(2): 421-436.
 35. Khattri, S.D., and M.K., Singh, 1999. Colour removal from dye wastewater using sugar cane dust as an adsorbent. *Adsorption Science and Technology*, 17: 269–282.
 36. Mahalakshmi, K., S.K., Suja, K., Yazhini, S., Mathiya, and G. J., Kalaivani, 2014. A novel approach to investigate adsorption of crystal violet from aqueous solutions using peels of annona squamosal. *Iranica Journal of Energy and Environment*, 5(2): 113-123.
 37. Ahmad, R., 2009. Studies on adsorption of crystal violet dye from aqueous solution onto coniferous pinus bark powder (CPBP). *Journal of Hazardous Materials*, 171: 767–773.
 38. Fu, J., Z., Chen, M., Wang, S., Liu, J., Zhang, and Q., Xu, 2015. Adsorption of methylene blue by a high-efficiency adsorbent (polydopamine microspheres): kinetics, isotherm, thermodynamics and mechanism analysis. *Chemical Engineering Journal*, 259: 53-61.
 39. Ho, Y.S., and G., McKay, 1999. Pseudo-second order model for sorption processes. *Process Biochemistry*, 34: 451–465.
 40. Patil, S., V., Deshmukh, S., Renukdas, and Patel, N., 2011. Kinetics of adsorption of crystal violet from aqueous solutions using different natural materials. *International Journal of Environmental Sciences*, 1(6): 1116-1134.
 41. Guo, J.Z., B., Li, L., Liu, and K., Lv, 2014. Removal of methylene blue from aqueous solutions by chemically modified bamboo. *Chemosphere*, 111: 225–231.
 42. Liu, Y., 2009. Is the Free Energy Change of Adsorption Correctly Calculated? *Journal of Chemical & Engineering Data*, 54: 1981–1985.
 43. Ardejani, F. D., K., Badii, N. Y., Limaee, S. Z., Shafaei, and A. R., Mirhabibi, 2008. Adsorption of Direct Red 80 dye from aqueous solution onto almond shells: Effect of pH, initial concentration and shell type. *Journal of hazardous materials*, 151(2-3): 730-737.
 44. Kumar, M., and R., Tamilarasan, 2013. Modeling studies for the removal of methylene blue from aqueous solution using Acacia

- fumosa seed shell activated carbon. Journal of Environmental Chemical Engineering, 1: 1108–1116.
45. Ben Arfi, R., S., Karoui, K., Mougin, A., Ghorbal, 2017. Adsorptive removal of cationic and anionic dyes from aqueous solution by utilizing almond shell as bioadsorbent. Euro-Mediterranean Journal for Environmental Integration, 2 (1): 20-32.
46. Bajpai, S.K., and A., Jain, 2012. Equilibrium and thermodynamic studies for adsorption of crystal violet onto spent tea leaves (STL). Water Journal, 4: 52-71.
47. Kannan, C., N., Buvaneswari, and T., Palvannan, 2009. Removal of plant poisoning dyes by adsorption on Tomato Plant Root and green carbon from aqueous solution and its recovery. Desalination, 249: 1132–1138.
48. Khattri, S.D., and M.K., Singh, 2000. Colour removal from synthetic dye wastewater using a bioadsorbent. Adsorption Journal Of The International Adsorption Society, 120: 283–294.

Persian Abstract

DOI: 10.5829/ijee.2018.09.04.05

چکیده

در این پژوهش، رنگ کاتیونی کریستال ویوله (CV) با استفاده از چوب پوسته آرگان (ARS) و پوسته بادام (ALS)، به عنوان جاذب‌های زیستی ارزان قیمت و سازگار با محیط زیست، حذف گردید. پارامترهای موثر در جذب CV بر روی هر یک از جاذب‌ها، زمان تماس (۵ تا ۱۸۰ دقیقه)، میزان جاذب (۰/۲ تا ۲ گرم)، pH محلول (۳-۱۱)، دما (۲۰-۵۰ °C) و غلظت رنگ اولیه (۵۰-۵۰۰ mg.L⁻¹) مورد ارزیابی قرار گرفت. مدلسازی نتایج حاصل از آزمایشات نشان می‌دهد که جذب CV بر روی هر دو ترکیب زیستی از سینتیک شبه درجه دو پیروی کرده و به طور کامل با ایزوترم لانگ‌مویر مطابقت دارد. همچنین، در دمای ۴۰ °C، جذب CV بر روی ALS با حداکثر جذب ۵۱/۹۹ mg.g⁻¹ بهتر از ARS با میزان ۳۷/۳۲ mg.g⁻¹ می‌باشد. محاسبات ترمودینامیکی نشان می‌دهد که جذب خودبخودی، گرماگیر و به صورت تصادفی در سطح تماس جامد-محلول رخ می‌دهد. ظرفیت جذب رنگ با استفاده از ALS و ARS نتایج بهتری را در مقایسه با سایر ترکیبات زیستی که تا به حال مورد مطالعه قرار گرفته‌اند، نشان می‌دهد. بنابراین، ترکیبات زیستی ALS و ARS می‌توانند به عنوان یک جاذب زیستی ارزان و سازگار با محیط زیست در نظر گرفته شوند.
